Self-assembly of Choline based Surface Active Ionic Liquids and Concentration dependent Enhancement in Enzymatic Activity of Cellulase in Aqueous Medium

Manpreet Singh,[a] Gurbir Singh,[a] Harmandeep Kaur,[a] Muskan,[a] Sugam Kumar,[b] Vinod Kumar Aswal,[b] Tejwant Singh Kang[a,*]

[a]*Department of Chemistry, UGC-centre for Advance Studies – II, Guru Nanak Dev University, Amritsar, 143005, India.*

[b]*Solid State Physics Division, Bhabha Atomic Research Centre, Mumbai 400085, India*

Electronic Supplementary Information

Annexure – S1

Synthesis of SAILs

Dissolve an equimolar amount of choline chloride and anionic salts (sodium lauroyl sarcosinate, sodium dodecylsulfate or sodium deoxycholate) to sufficient amount methanol (AR grade) in two different round bottom flasks (RBF). Mix the two solutions and stir the solution for 6h at 45 ^{o}C. Cool the solution to room temperature and evaporate methanol using rotary evaporator. To the obtained compound, put chloroform (AR grade) and stir the solution for 15 minutes. Allow the salt (NaCl) to settle and filter using Whatman filter paper. Dry the filtrate using rotary evaporator. Repeat the last step twice and collect the product. The obtained SAILs were dried under vacuum for 24 hours.

Annexure – S2

Cellulase Activity

Dinitrosalicylic acid (DNS) suger assay test employing sodium carboxymethyl cellulose (Na CMC) was used to investigate the activity of cellulase in the aqueous solution of choline-based SAILs. The method used to prepare DNS reagent has been described in the literature elsewhere.[1] Cellulase in the different SAIL solutions (133 µl) and 1 % (w/v%) Na CMC (1200 µl) solutions was incubated at 45 ^{o}C for 20 minutes and then 266 µl of DNS reagent was added. The obtained solution was heated at 90 ^{o}C for 5 minutes on a water bath. The color of the solution changed to deep red owing to the reduction of nitro group of DNS to the amino group by the action of sugar produced during hydrolysis of Na CMC. This color was stabilized by adding 133 µl of 40% Rochelle salt and the solutions were cooled to room temperature. Then the absorbance at 546 nm was recorded and the concentration of sugar formed was calculated by making use of the standard calibration curve obtained using different concentrations of glucose obtained via DNS analysis. Mathematically, the activity of cellulase was calculated using the equation:[2]

$$EA = \frac{c}{M \times t \times V} \quad \textbf{(4)}$$

where EA is enzyme activity, c and M are the concentration and molecular weight of sugar, respectively, t is the incubation time and V is the volume of the enzyme used.

Annexure – S3

Equations used to calculate effectiveness of surface tension reduction (Π_{cmc}) and maximum surface adsorption (τ_{max}).

$$\Pi_{cmc} = \gamma_o - \gamma_{cmc} \quad \textbf{(1)}$$

$$\tau_{max} = 10^{23}/N_A * A_{min} = \frac{-1}{nRT}(\partial\gamma/\partial lnC)_T \quad \textbf{(2)}$$

Annexure – S4

Fitting models used to interpret SANS experimental data.

In SANS, the intensity of the scattered neutrons measured as a function of Q (magnitude of wave vector transfer) is proportional to the coherent differential scattering cross-section per unit volume ($d\Sigma/d\Omega$). For a system of monodispersed particles dispersed in a medium, it can be given by

$$\frac{d\Sigma}{d\Omega}(Q) = nV^2\left(\rho_p - \rho_s\right)^2 P(Q)S(Q) + B \quad (1)$$

where n is the number density and V is particle volume. ρ_p and ρ_s are scattering length densities of particles and solvent, respectively. $P(Q)$ is intraparticle structure factor, which depends on the structural parameters (shape, size and size distribution) of the scatterers. $S(Q)$ is interparticle structure factor which is related to the inter-particle interactions and can be approximated to unity for dilute samples. B is a constant term representing incoherent background and decides the scattering at the highest Q value.

The $P(Q)$ of ellipsoidal particle can be written as:

$$P(Q) = V^2(\rho_p - \rho_s)^2 \int_0^1 [F(Q,\mu)]^2 d\mu \quad \textbf{(3)}$$

where $F(Q, x) = \frac{3(sin\ x - x\cos x)}{x^3}$ in this $x = Q\left[a^2\mu^2 + b^2\left(1-\mu^2\right)\right]^{\frac{1}{2}}$

where a and b represent the semimajor and semi minor axes for prolate ellipsoid shape, μ is the cosine of the angle between the direction of major axis and wave vector transfer Q.

The polydispersity in the size distribution of particles is incorporated using the following integration

$$\frac{d\Sigma}{d\Omega}(Q) = \int \frac{d\Sigma}{d\Omega}(Q,R) f(R) dR + B \ ,$$

where $f(R)$ is the size distribution of the vesicles and usually accounted by a log-normal distribution as given by

$$f(R) = \frac{1}{\sqrt{2\pi} R\sigma} \exp\left[-\frac{1}{2\sigma^2} \left(\ln \frac{R}{R_{med}} \right)^2 \right] ,$$

where R_{med} is the median value and σ is the standard deviation (polydispersity) of the distribution. The mean radius (R_m) is given by $R_m = R_{med} \exp(\sigma^2/2)$.

Annexure – S5

Different parts Cellulase complex

Cellulase in actual is a cellulase complex, which includes three different enzymes: (i) endo-glucanase, (ii) exo-glucanase and (*iii*) β-glucosidase responsible for the complete breakdown of cellulose into glucose.[3] The endo-glucanase causes random hydrolysis of β-1,4-glucosidic bonds of cellulose resulting in relatively smaller chains of cellulose with enhanced solubility, which undergoes rapid hydrolysis. The repeated action of endo-glucanase yields cellobiose and cellotriose as the final product. The exo-glucanase produce cellobiose as major product whereas the multiple hydrolysis of cellulose through non-reducing ends of exo-glucanse also yields glucose molecules. The main structural difference between exo- and endo-glucanase is the morphology of their active sites. Active site of endo-glucanase have tunnel like morphology,

whereas exo-glucanase have open cleft-like active site owing to the absence of loops covering the carboxyl terminal of *β*-barrel. Third enzyme *i.e., β*-glucosidase is responsible for the conversion of cellobiose and short chain oligo-glucosides into glucose. The enzymes of cellulase complex work in conjunction with each other and there exists a synergism between them which cause high rate of hydrolysis of cellulose.[4]

Figures

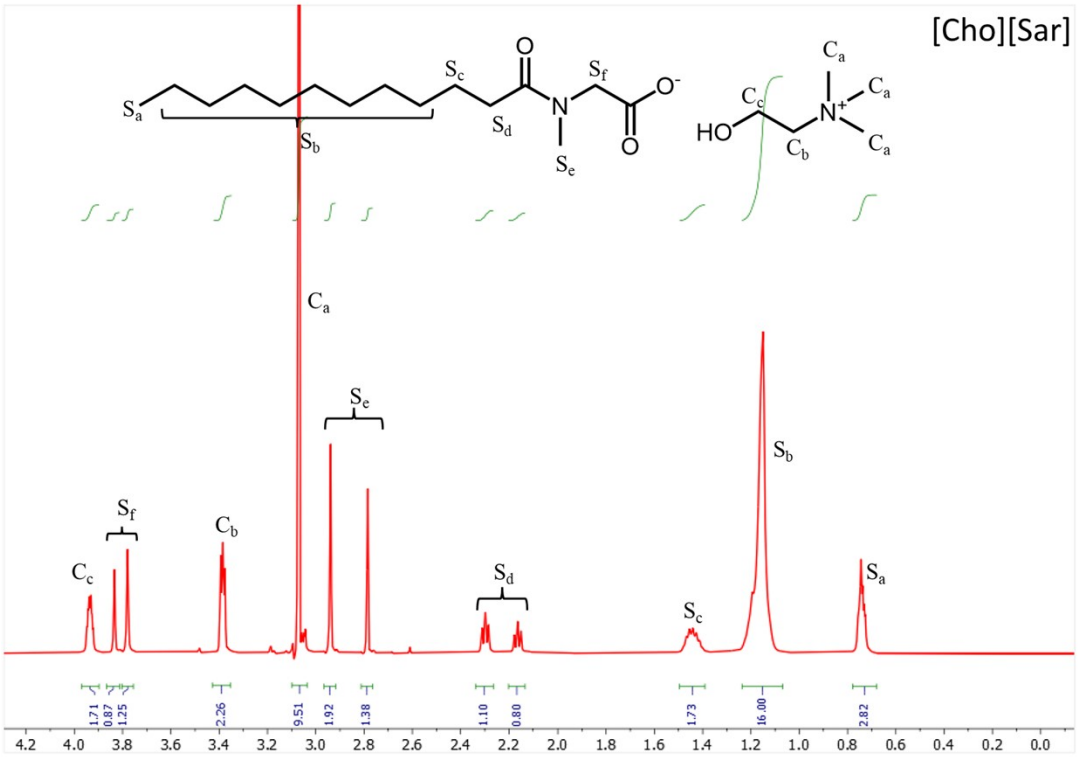

Figure S1: [1]H-NMR spectra of [Cho][Sar]

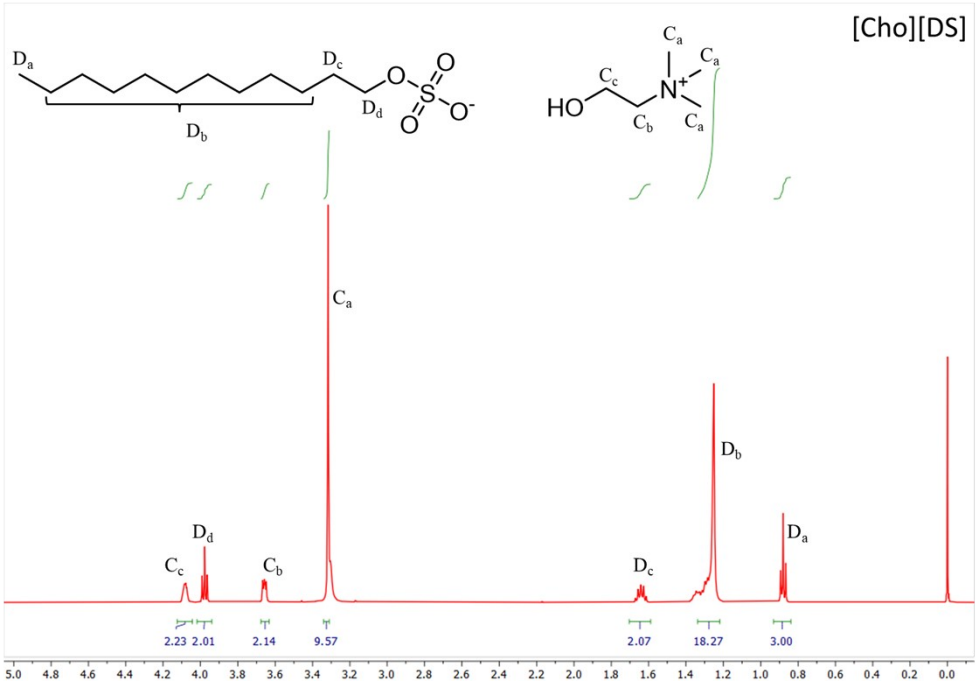

Figure S2: ^{1}H-NMR spectra of [Cho][DS]

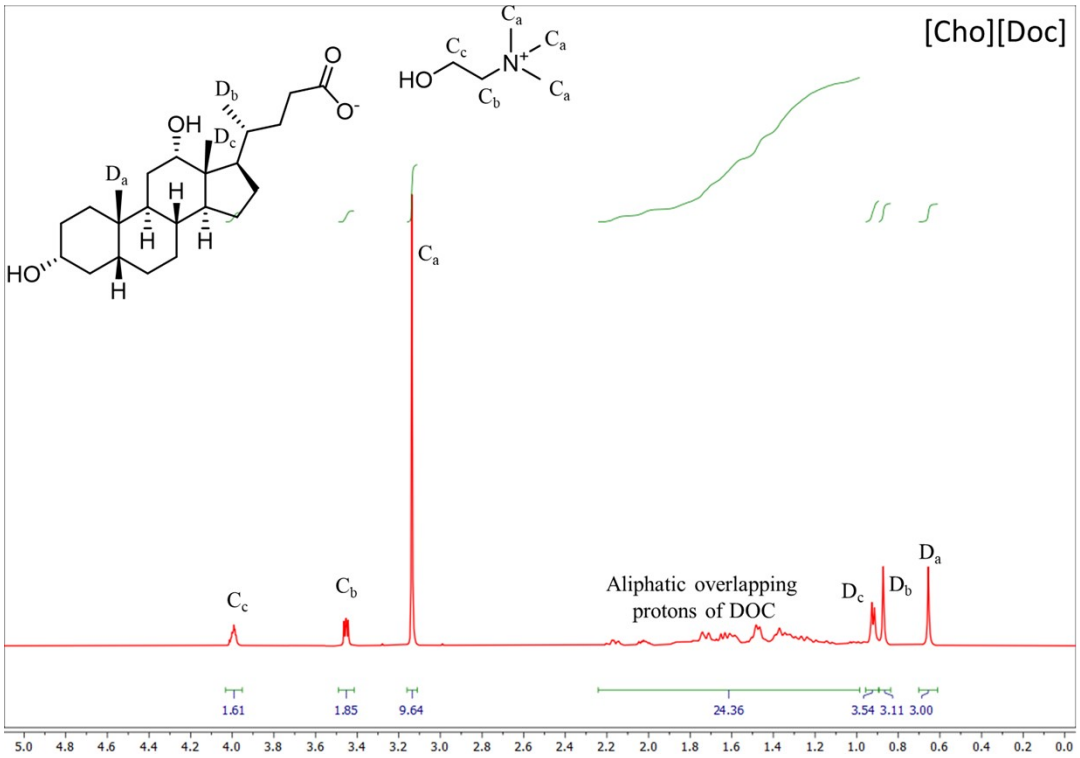

Figure S3: ^{1}H-NMR spectra of [Cho][Doc]

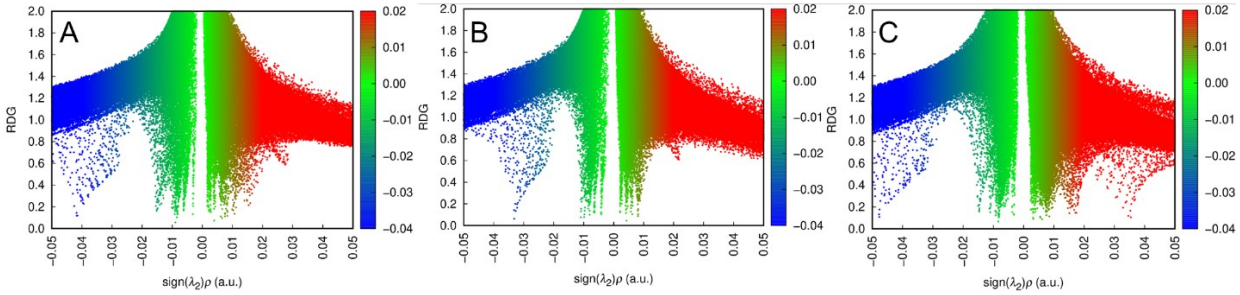

Figure S4 (A-C): 2D RDG filled plot for (A) [Cho][Sar], (B) [Cho][DS] and (C) [Cho][Doc].

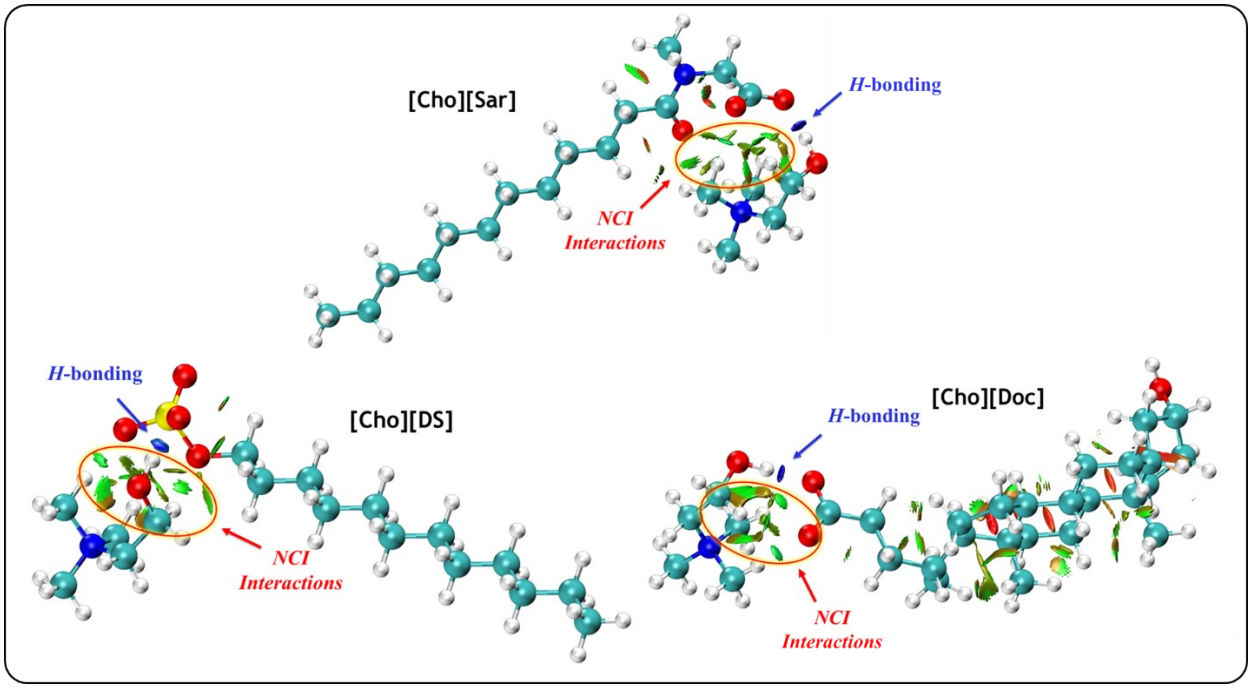

Figure S5: NCI iso-surfaces visualization for the SAILs under investigation.

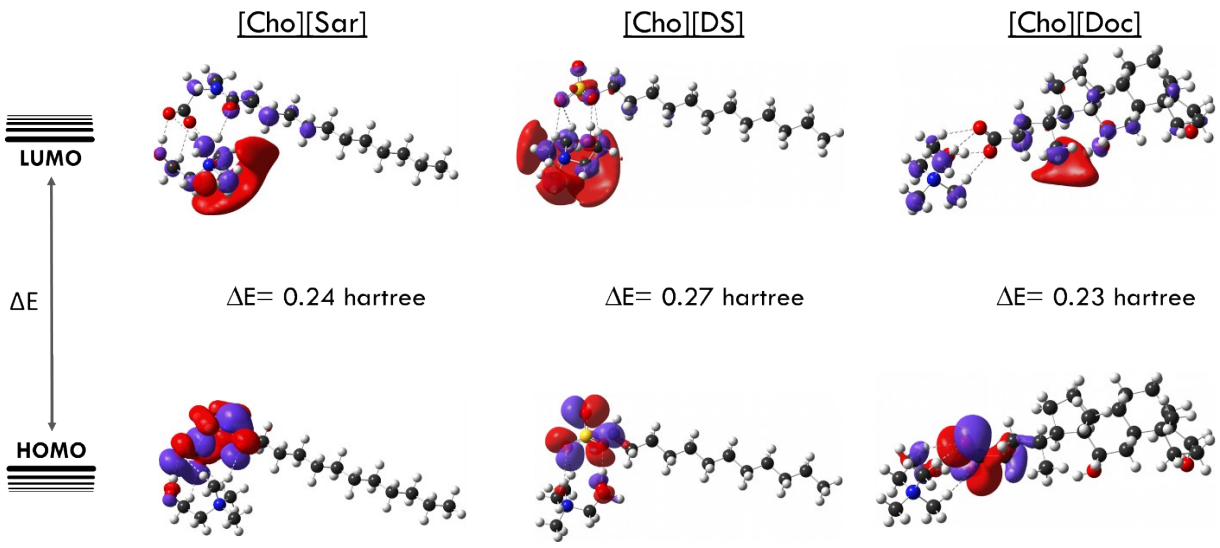

Figure S6: Visualization of HOMO-LUMO for Choline based SAILs along with the band gap.

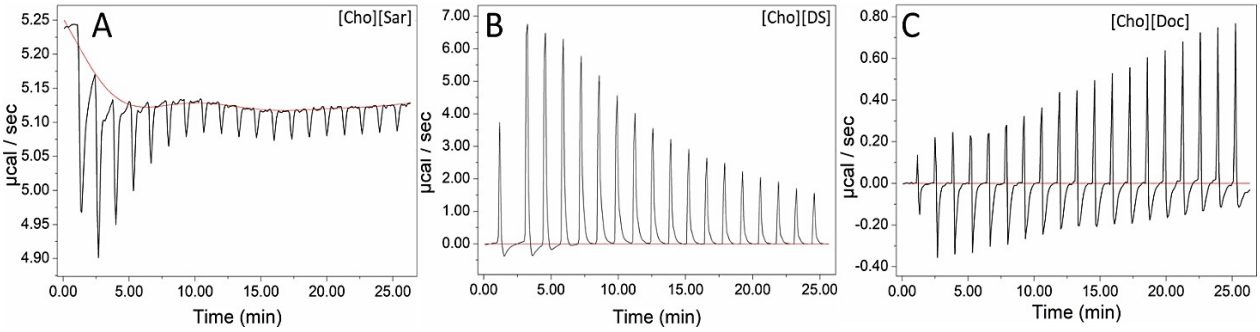

Figure S7 (A-C): Differential power plots for (A) [Cho][Sar], (B) [Cho][DS] and (C) [Cho][Doc].

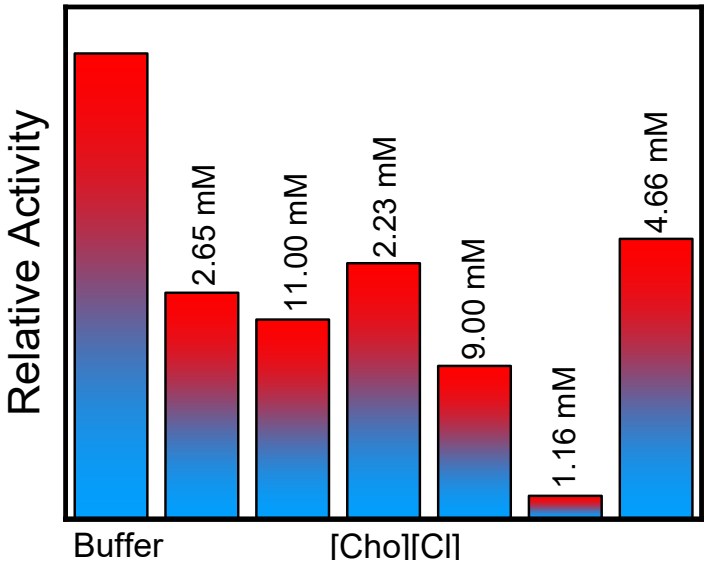

Figure S8: Relative activity of cellulase in aqueous solution of Choline chloride at concentrations equal to below (0.5) and above (2) *cmc* of different choline-based SAILs under investigation as compared to that observed in buffer.

Table S1: Various physicochemical parameters of choline-based SAILs calculated from DFT calculations.

Physiochemical Parameters	**[Cho][Sar]**	**[Cho][DS]**	**[Cho][Doc]**
Chemical potential (μ)	-0.12	-0.14	-0.11
Electronegativity (χ)	0.12	0.14	0.11
Chemical hardness (η)	-0.12	-0.14	-0.11
Softness (S)	-4.17	-3.57	-4.54
Global electrophilicity index (ω)	0.50	0.5	0.50

Refrences

1 B. Anita, A. J. Thatheyus and D. Ramya, Biodegradation of Carboxymethyl Cellulose using Aspergillus flavus, *Sci. Int.*, **1**, 85–91.
2 P. S. Gehlot, A. Kulshrestha, P. Bharmoria, K. Damarla, K. Chokshi and A. Kumar, Surface-Active Ionic Liquid Cholinium Dodecylbenzenesulfonate: Self-Assembling Behavior and Interaction with Cellulase, *ACS Omega*, 2017, **2**, 7451–7460.
3 D. B. Wilson, in *Encyclopedia of Microbiology (Third Edition)*, ed. M. Schaechter, Academic Press, Oxford, 2009, pp. 252–258.
4 J. K. Saini, R. Saini and L. Tewari, Lignocellulosic agriculture wastes as biomass feedstocks for second-generation bioethanol production: concepts and recent developments, *3 Biotech*, 2015, **5**, 337–353.